165

Egypt. J. Chem. **Vol. 68**, No. 4 pp. 195 - 204 (2025)

Egyptian Journal of Chemistry

http://ejchem.journals.ekb.eg/

Zn-MOFs/CNTs Composites: Fast and Effective Heavy Metal Ion Removal from Wastewater

Marwa. S. Saleh[1,3,4], Mohamed. O. Abdel-Salam[2,3,4], Raed. M. Hegazey[3,4], Mona El-Sayed[3,4], Taeho Yoon[5], Yaser. M. Moustafa[3,4], Mostafa M.H.Khalil[1]*

[1] *Chemistry Department, Faculty of Science, Ain Shams University, 11566 Abbassia, Cairo, Egypt.*
[2] *Department of Chemistry, School of Science and Engineering, the American University in Cairo, Cairo, 11835, Egypt*

[3] *Analysis and Evaluation Department, Egyptian Petroleum Research Institute (EPRI), 1 Ahmed El Zomor st., Nasr City, Cairo, 11727, Egypt*

[4] *Central Analytical Laboratories, Nanotechnology Research, Egyptian Petroleum Research Institute (EPRI), 1 Ahmed El Zomor st., Nasr City, Cairo, 11727, Egypt*

[5] *Department of Chemical Engineering, Kyung Hee University, Yongin-si, Gyeonggi-do, 17104 Republic of Korea*

Abstract

The subsistence of heavy metal ions, including Cu^{2+} and Pb^{2+}, raises substantial concerns due to their potential toxicity to both the environment and human health. In this study, a novel adsorbent, the Metal-organic framework based on zinc (Zn-MOFs), incorporated with carbon nanotubes (CNTs), denoted as Zn-MOFs/CNTs, were synthesized using a room-temperature precipitation method for the efficient removal of heavy metals. The Zn-MOFs/CNTs composites were meticulously characterized using a range of analytical techniques such as Fourier transform infrared spectroscopy (FT-IR), X-ray diffraction (PXRD), field emission scanning electron microscopy (FE-SEM), and high-resolution transmission electron microscopy (HR-TEM). The effectiveness of Zn-MOFs/CNTs in removing Cu^{2+} and Pb^{2+} ions from water was assessed, considering adsorption time and initial ion concentration as key parameters. The results demonstrated the remarkable performance of Zn-MOFs/CNTs, achieving removal efficiencies exceeding 98% for Pb^{2+} and 93% for Cu^{2+} within a 12-minute timeframe. The maximum adsorption capacities determined (qm) by Langmuir isotherms were 1620 mg/g for Cu^{2+} and 1480 mg/g for Pb^{2+} at 303 K. The study concludes by providing recommendations and suggesting future directions for enhancing the application of MOFs-functionalized/CNTs in water treatment and reuse.

Keywords: Metal-organic framework (MOFs); Wastewater treatment; CNTs; Heavy metals; and Adsorption

1. Introduction

Ensuring public health, and eliminating metal ions from the water supply remains a critical challenge. The swift advancement of industrial activities has led to the deliberate and accidental release of contaminants, including heavy metal ions, from factories. This has significantly contributed to the water pollution problem, posing a threat to the health of living organisms [1]. Heavy metal ions enter the water supply system through a variety of mechanisms, including pipe dissolving, radioactive waste from nuclear power plants, fertilizers, and mining. Hence, securing access to safe drinking water is fundamental to maintaining a healthy lifestyle [2]. Consequently, an assortment of different techniques has been utilized to remove metal ions from aqueous solutions, including coagulation, membrane separation, and ion exchange. Yet, these methods encounter obstacles such as elevated operational expenses, incomplete removal, and the possible creation of secondary hazardous pollutants [3]. The adsorbent plays a crucial role in the adsorptive removal of ions, offering a straightforward and rapid separation process. This efficient and cost-effective method has been extensively employed in water treatment [4]. Adsorption capacity and selectivity in the adsorption process are heavily influenced by the adsorbents executed. The limited adsorption capabilities and suboptimal selective sorption properties of typical adsorbents such as activated carbon [5], zeolites [6], and

_____

_____

natural fibres [7]. Consequently, the creation of innovative adsorbents that are both highly efficient and selective for specific pollutants has captured public attention and currently stands as the central priority in the field of adsorption. In this context, recent investigations have explored the potential of newly identified materials including graphene [8], carbon nanotubes (CNTs) [9], and Metal-Organic Frameworks (MOFs) [10] as adsorbents for capturing heavy metals. These materials have demonstrated significant potential for use in water purification.

The CNTs have exceptional mechanical, thermal, and electrical characteristics as well as unique adsorption capabilities, making them one of the best adsorbents for the adsorption of inorganic and organic compounds in aqueous systems [8] [9]. MOFs represent an innovative class of crystalline porous materials for adsorption [13], constructed through the strategic assembly of suitable organic ligands and metal ion units, which form interconnected three-dimensional frameworks. MOFs offer significant benefits as adsorbent materials, owing to their diverse composition and structure, exceptionally high surface areas, molecular-sized voids, superior chemical and thermal stability, and the straightforward functionalization of their pores or external surfaces. Consequently, they are highly advantageous for adsorption [15] [14] and separation processes [16]. Herein, we engineered CNTs embellished with Zn-MOFs directly grown on their framework to synergistically boost the adsorption efficiency of Cu^{2+} and Pb^{2+} ions from wastewater. The impact of variables including contact duration, and levels of lead and copper ions in the solutions, was assessed. This study demonstrates that Zn-MOFs/CNTs are highly effective in extracting heavy metal ions from water, making them suitable for advanced water purification.

2. Materials and Methods

2.1 Materials
All the starting reagents, Terephthalic acid, Zinc acetate dehydrate Zn $(OAC)_2.2H_2O$ 98%, N, N-Dimethyl methanamide (DMF) 99.8%, Triethyl amine 99%, Ethanol absolute 99%, Copper Sulphate $(CuSO_4.5H_2O)$, Lead Acetate were purchased from LOBA CHEME PVT.LTD. Carbon Nanotubes (CNT) were obtained from the Egyptian Petroleum Research Institute (EPRI). Deionized water (18.2 MΩcm) was prepared using a water pro-Labconco deionization system, in Central Analytical Laboratories (EPRI). All reagents, of analytical grade, were used as received.

2.2 Preparation of Zn-MOFs

Zn-MOFs nanomaterials were prepared at room temperature by adding Zn acetate (25 mg), and terephthalic acid (85 mg) into the mixture containing DMF (1400μm), ethanol (600μm), Triethyl amine (42μm) as capping agent, Subsequently, the blended mixture was agitated for 2.5 hours. The product underwent filtration and was subsequently rinsed three times with ethanol (20 mL each time). Following this, the white precipitate was dried overnight in a vacuum oven at 60 °C for 24 hours.

2.3 Preparation of Zn-MOFs/CNTs nanocomposite

Zn-MOFs with CNTs were prepared at room temperature with Zn acetate (25 mg), Terephthalic acid (85 mg), and dissolved in DMF (1400μm), Ethanol(600μm), Triethyl amine (42μm) as capping agent, then added CNTs (10 mg) suspended in Ethanol (5 ml), Afterwards, the mixed solution was agitated for 2.5 hours. The result was filtered thrice with each wash of 20 mL ethanol. A vacuum oven was used to dry the grey goods overnight at 60 °C. The schematic illustration for Zn-MOFs/CNTs nanocomposite is presented in Fig.1.
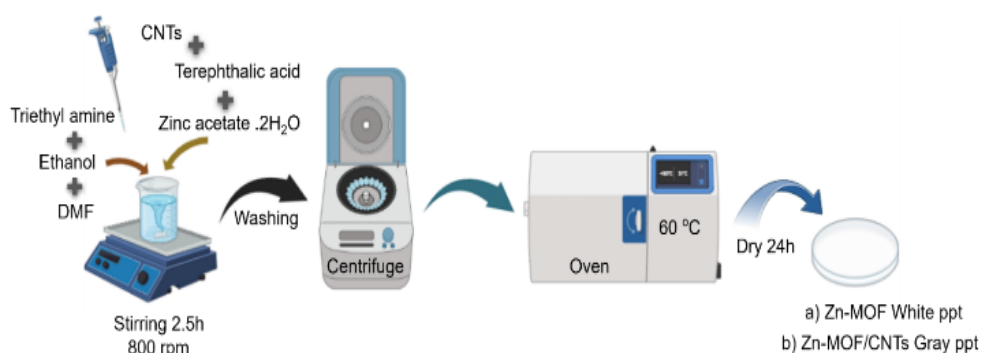

Fig. 1: Schematic illustration for Zn-MOFs/CNTs prepared at room temperature.

_____

_____

2.4 Characterization techniques of the prepared materials

Various characterization techniques were employed to identify the produced nanocomposite materials. The crystal structure of the synthesized materials was characterized through X-ray diffraction (XRD). Phase identification was performed using a Pan analytical X'PERT PRO MPD X-ray powder diffract meter (Cu Kα radiation at λ=1.5418 A^o with a rating of 40 KV and 40 mA). Diffraction patterns were captured at ambient temperature across an angular range from 10° to 80° 2θ, with a step size of 0.02° 2θ and a scan step duration of 0.4 seconds. Fourier transform infrared (FT-IR) spectroscopy (PERKIN ELMER, USA), employing attenuated total reflection (ATR) over a range of 4000 and 400 cm^{-1}, was utilized to analyze the functional groups in the synthesized nanocomposite materials.

Field emission-scanning electron microscopy (FE-SEM, Sigma 300VP) was employed to elucidate the structural and morphological details of the samples. Operating at a voltage of 30 kV and magnifications ranging from 14x to 1,000,000x, SEM images were captured. For these images, particles were mounted on aluminum SEM stubs with carbon tape at room temperature and subsequently coated with a thin layer of gold under vacuum conditions to improve conductivity. Transmission electron microscopy (TEM, JEOL-JEM 2100, Japan) was employed to capture images of Zn-MOFs and Zn-MOFs/CNTs. These images were obtained under vacuum conditions on a copper-coated carbon grid, utilizing an operating voltage of 200 kV. All samples were measured via adsorption-desorption of N$_2$ gas at 77 K)) using its patent method of AFSM (Advanced Free Space Measurement) to get the most accurate measurements. The Brunauer-Emmett-Teller (BET) method, utilizing the BELSORP MINI X models, is employed to ascertain the specific surface area. The concentration of the studied metals was measured before and after the treatment by atomic absorption spectrometry using flame atomic absorption spectrometer ZEE-nit 700 P analytic Jena Company, Germany

2.5 Adsorption studies

A set of batch adsorption tests was conducted to evaluate the effectiveness of Zn-MOFs/CNTs in removing specific heavy metal ions (i.e., Cu^{2+} and Pb^{2+} ions) from aqueous solutions.
The adsorption studies assessing the removal efficiency of Zn-MOFs and Zn-MOFs/CNTs composites, expressed in Eq. 1

$$R(\%) = \left({C_i - C_e}/{C_e} \right) \times 100 \qquad (1)$$

Where R (%) is the removal efficiency and q_e (mg/g) the adsorption capacity at equilibrium, C_i and C_e (mg/L) are the initial and equilibrium concentrations of Cu^{2+} and Pb^{2+} ions, correspondingly. To achieve this, 0.5 g of Zn-MOFs/CNTs were introduced into 100 mL of aqueous solutions containing different concentrations of the targeted heavy metals and agitated at ambient temperature. Temperature and time of stirring were adjusted at 25 ^{o}C and 30 min, respectively. After the finalization of the preconcentration procedure, Zn-MOFs/CNTs catalysts were separated from the sample solution using filtration. The concentration of residual metal ions in each stock solution was measured using atomic absorption spectrometry. The amount of copper adsorbed using the Zn-MOFs/CNTs catalyst was determined by measuring the difference between the initial and final concentrations of Cu in the sample solution

3. Results and Discussion

Adsorbent characterization

The X-ray diffraction (XRD) patterns depicted in Fig. 2 validate the crystal structure of the synthesized Zn-MOFs and Zn-MOFs/CNTs composites. The XRD pattern of the pristine CNTs displayed a wide diffraction peak at 26° and 43°, which were attributed to *(h k l)* values of (0 0 2) and (1 0 0) respectively, these characteristic peaks refer to the amorphous carbon [16]. However, the highly crystalline framework of the synthesized Zn-MOFs was confirmed by diffraction peaks displaying four main specific peaks which were observed at 2θ values around 8.83, 9.85, 19.25, and 19.75 degrees. The intensity of the spectrum for Zn-MOFs/CNTs was approximately as well as their parent materials (Zn-MOFs), indicating that Zn-MOFs were successfully combined with CNTs. The Zn-MOFs/CNTs composites had a comparable pattern to Zn-MOFs, with the addition of carbon nanotubes resulting in changes to the microstructure or a reduction in the crystallinity of the MOFs. Remarkably, no substantial shift in the peak location was found. Furthermore, the high intensity of Zn-MOFs/CNTs peaks resulted in the absence of the distinctive carbon nanotubes peak within the 2θ range of 27–26°. Besides, the magnitude of the distinctive peaks in the Zn-MOFs/CNTs composite structure was diminished compared to the pure Zn-MOFs sample. The decreased concentration of the metal-organic framework, influenced by the presence of carbon nanotubes, accounts for this reduction.
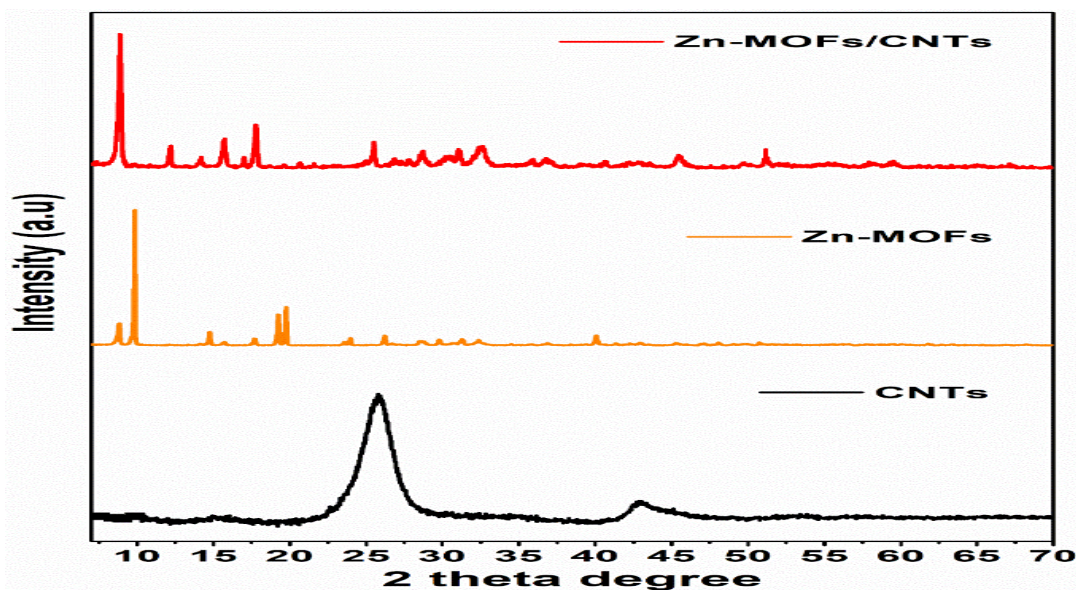
_____

Fig. 2. Stimulated XRD pattern of the prepared materials: (a) CNTs, (b) Zn-MOFs, (c) Zn-MOFs/CNTs

The elucidation of Zn-MOFs and Zn-MOFs/CNTs was confirmed from infrared (IR) spectroscopy (Fig. 3). The FT-IR patterns of Zn-MOFs and Zn-MOFs/CNTs were similar to the literature [17][18][19]. As evident from the spectrum, the broad bands of Zn-MOFs at 1364, and 1572 cm^{-1} are due to the (O = C – O) carboxylic group linked to Zn exhibiting both symmetric and asymmetric stretching vibrations. The adsorption band around 3737 cm^{-1} contributes to the O-H stretching vibration of water molecules adsorbed within the Zn-MOFs structure. Meanwhile, the broad band at 3126 cm^{-1} arises from the symmetric stretching of N-H bonds. The composite's internal structure remained substantially inherent after adding CNTs, with no appreciable alteration. The peaks at 1624 cm^{-1} and 1254 cm^{-1} Within the low-frequency domain, there are N-H bending vibrations and aromatic amines, respectively. The bands identified within the 600 and 1600 cm^{-1} were attributed to phenyl functional groups. These groups encompassed a C=C band at 1508 cm^{-1} and C-H deformation bands at 1159, 1018, 885, and 751 cm^{-1} with a faint signal at 3070 cm^{-1}. The FTIR spectra for Zn-MOFs/CNTs nanocomposites displayed a characteristic peak at 3604cm^{-1}, indicative of the stretching vibrations associated with C-OH and O=C-OH within the carboxyl functional groups present on the acid-modified CNTs.
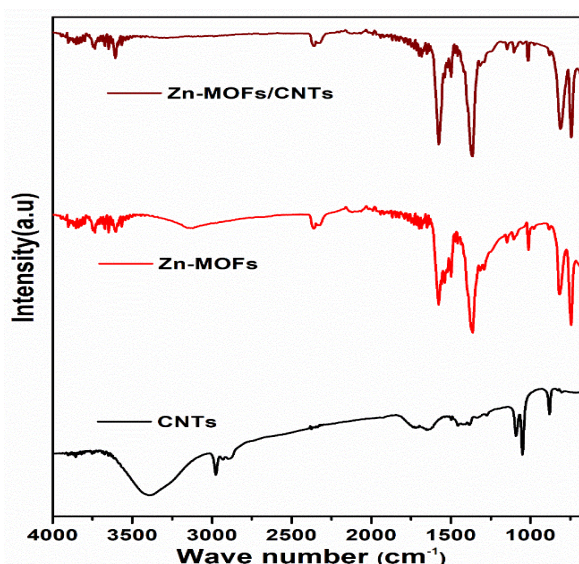

Fig. 3. FTIR spectra of the prepared samples: (a) CNTs, (b) Zn-MOFs, (c) Zn-MOFs with CNTs.

The surface morphology and microstructural characteristics of the synthesized materials were assessed through analyses performed with field-emission scanning electron microscopy (FE-SEM) and transmission electron microscopy (TEM). Through the utilization of transmission electron microscopy, we obtained high-resolution images of the synthesized crystalline Zn-MOFs and Zn-MOFs/CNTs composite materials (Fig. 4a,b). The synthesized pure Zn-MOFs materials exhibited the distinct features of a crystalline multi-dimensional morphological structure, demonstrating excellent dispersibility. Presently, the molecular interaction of the organic ligand is diminished or eliminated, while its deprotonation is intensified, thereby facilitating the crystallization process in the aqueous solution. Images of the Zn-MOFs/CNTs composite demonstrated the accurate integration and distribution of carbon nanotubes within the Zn-MOFs structure The FE-SEM images for Zn-MOFs/CNTs are illustrated in Fig. 4c. The Zn-MOFs display a versatile multi-dimensional form, a result of the optimal interaction between the metal and the ligand. Besides, there is no substantiated evidence of particle agglomeration, which enhances the refinement of the catalytic characteristics of the samples [20]. The addition of CNTs into the Zn-MOFs maintains the original structure of Zn-MOFs (Fig.4b, c).
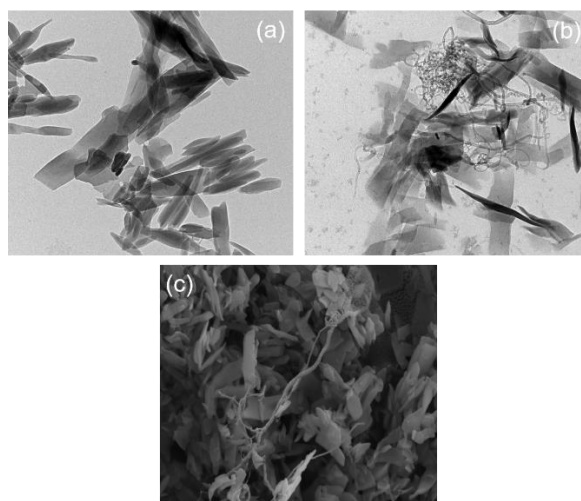

Fig. 4. Transmission electron microscope (TEM) and Scanning electron microscope (SEM) images: (a) TEM image of Zn-MOFs, (b) TEM image of Zn-MOFs/CNTs, and (c) SEM image of Zn-MOFs/CNTs.

Fig. 5. illustrates the nitrogen adsorption-desorption isotherms at 77 K for the produced samples. Both materials exhibited notable N2 uptake at low relative pressures (P/P0 < 0.1), displaying a type III isotherm with an H4 hysteresis loop, indicating the presence of a microporous structure [21]. Both Zn-MOFs and Zn-MOFs/CNTs demonstrate a BET surface area of 5.03 and 15.46 m² g^{-1}, respectively. Despite having a low surface area obtained from BET, the Zn-MOFs/CNTs found to possess better adsorption activity, but still higher than the Zn-MOFs alone, This could be because BET typically demands substantial sample quantities to obtain precise statistical outcomes. When samples are insufficient, the results can be significantly skewed. Consequently, BET has been unable to deliver high-throughput analyses necessary for the swift advancement of MOFs [22].
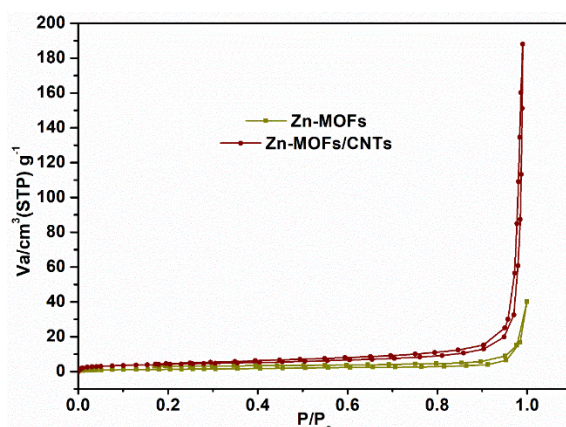

Fig. 5. N$_2$ adsorption-desorption isotherms of the Zn-MOFs and Zn-MOFs/CNTs samples.

Selective adsorption behaviors Zn-MOFs/CNTs.

A series of batch sorption experiments were conducted using aqueous solutions containing heavy metal ions like Pb^{2+} and Cu^{2+}. These tests aimed to evaluate the capacity and performance of Zn-MOFs/CNTs in selectively adsorbing these ions.

_____

Effect of Time

   The optimum contact time for the Cu^{2+} uptake by Zn-MOFs, CNTs, and the Zn-MOFs/CNTs composite was ascertained by altering the contact time intervals. This approach aimed to explore the removal process speed and establish the optimal duration for conducting all subsequent experiments. Fig. 6a illustrates how contact time influences the uptake capacity of the Zn-MOFs/CNTs composite. This experiment utilized a 25 ml solution with an initial Cu^{2+} concentration of 500 ppm, a dosage of 20 mg, and was conducted at a temperature of 303 K. It was observed that the percentage of Cu^{2+} removed grew as the contact time lengthened, reaching equilibrium at 12 minutes. The swift initial absorption of metal ions can be attributed to the abundance of vacant sites available for binding. Subsequently, the remaining free metal ions encounter difficulty in adsorption due to the repulsive forces between the free ions and those already adsorbed (Fig. 6b).
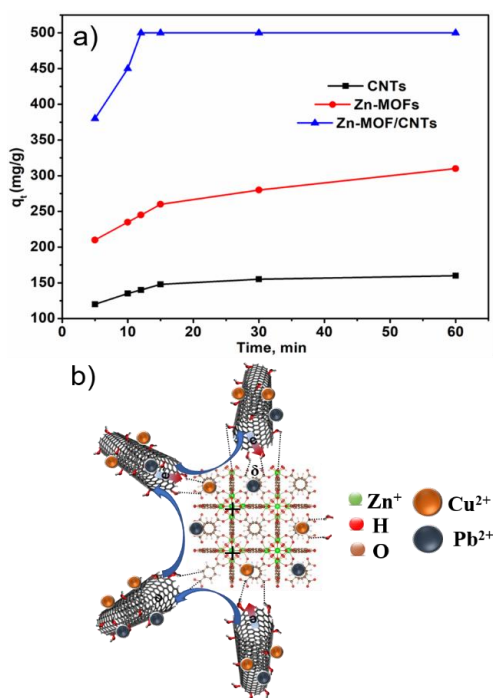

Fig. 6. a) Cu adsorption capacity curves of CNTs, Zn-MOF and Zn-MOF/CNTs composite at different time intervals using 5 mg adsorbate and 25ml of the highest used Cu concentration solution, 500 ppm, b) Schematic structure of the proposed adsorption of metals ions.

Adsorption kinetics

   The kinetic adsorption studies of Cu^{2+} ions by Zn-MOFs/CNTs composite were examined using a pseudo-second-order kinetic model with the Eq. (2):

$$\frac{t}{q_t} = \frac{1}{k_2 q_e^2} + \frac{t}{q_e} \qquad (2)$$

Where; qe = amount of metals adsorbed at equilibrium (mg/g), qt =amount of metals adsorbed at a time, t (mg/g), and K$_2$ = pseudo-second-order reaction rate constant (g/mg min). As shown in Fig. 6a the removal capacity for Cu^{2+} ions on the Zn-MOFs/CNTs with time was achieved. The elimination of targeted ions occurs rapidly, and the maximum adsorption capacity is achieved within 12 min. The high coefficient of determination (R² > 0.9999) suggests that the pseudo-second-order model accurately describes the adsorption kinetics of Zn-MOFs/CNTs. This indicates that the sorption process is primarily driven by chemical adsorption (chemisorption) reactions, involving valence forces through electron sharing or exchange between the metal ions and the active sites on Zn-MOFs/CNTs. In chemisorption, the adsorption capacity is thought to be directly proportional to the number of active sites occupied on the adsorbent's surface (see Figure 6b) 23.

Effect of adsorbent weight

   Fig. 7 illustrates the impact of different dosages of Zn-MOFs/CNTs adsorbents on the efficiency of Cu^{2+} and Pb2+ ion removal. The findings indicate that, with all other conditions held constant, increasing the adsorbent dose from 10 mg to 40

_____

mg in a 25 ml solution of 500 ppm Cu^{2+} and Pb^{2+} leads to a higher adsorption efficiency. Specifically, the removal rate for Cu^{2+} ions rose from 81.02% to 98.06%, while for Pb^{2+} ions, it increased from 65.01% to 93.03%. When the adsorbent dosage was minimal, there was an abundance of ions relative to the available adsorption sites. Consequently, the likelihood of these sites being filled was elevated, leading to a high adsorption capacity. However, as the adsorbent dosage increased, more adsorption sites became accessible for the ions, thereby enhancing the removal ratio.
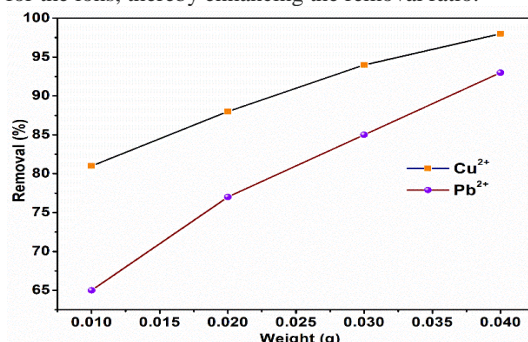

Fig. 7. Uptake efficiency of Zn-MOFs/CNTs at different weights from 10 to 40 mg adsorbate for high concentration 500 ppm, 25ml for (a) Cu^{2+}, and Pb^{2+} solution.

The effect of initial metal concentration

A series of batch experiments were carried out to explore how the initial metal concentrations impact the removal efficiency of Cu^{2+} and Pb^{2+} by Zn-MOFs/CNTs. The experiment was conducted under controlled conditions, with a constant contact time, dose (20 mg), temperature (303 K), and pH (7). The initial concentration varied between 50 and 600 ppm. The adsorption isotherm plots illustrating the uptake of Cu^{2+} and Pb^{2+} ions are shown in (Fig. 8a), and (Fig. 8b). The Zn-MOFs/CNTs material exhibited a progressive enhancement in its ability to adsorb Cu^{2+} and Pb^{2+}, with maximum capacities of 1620 mg g^{-1} and 1480 mg g^{-1}, respectively, observed at an initial concentration of 500 mg L^{-1}.
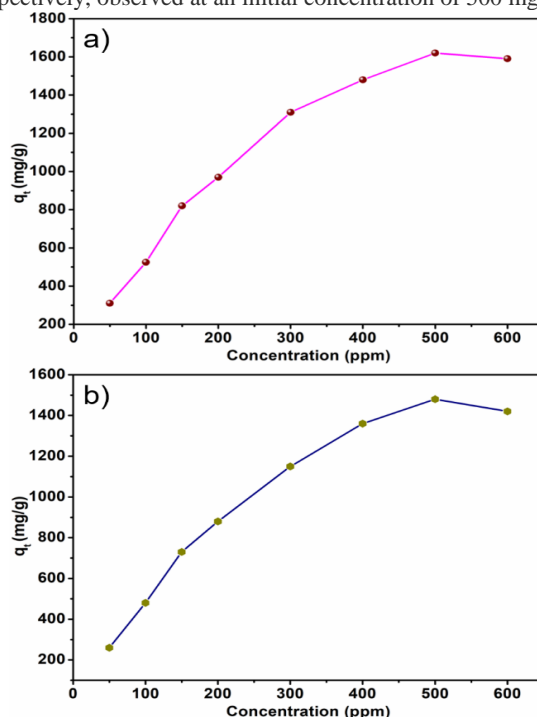

Fig. 8. The adsorption curves for the Zn-MOFs/CNTs at different initial concentrations: (a) Cu^{2+}, (b) Pb^{2+}.

Comparison with other MOFs-based adsorbents

Table 1 highlights the superior sorption capacity of Zn-MOFs/CNTs in removing Cu^{2+} and Pb^{2+} ions from water, exceeding the performance of other MOF-based adsorbents cited in previous research. As indicated in Table 1, the highest sorption capacities of Zn-MOFs/CNTs for Cu^{2+} and Pb^{2+} are greater than those reported for most other MOF-based adsorbents in the literature [23][24][25]. These findings confirm that Zn-MOFs/CNTs are highly effective adsorbents for the removal of Cu^{2+} and Pb^{2+} ions from contaminated water.

_____

Table 1. The compared results of the sorption capacity of Zn-MOFs/CNTs for Cu (II) ions, (b) Pb (II) ions with different absorbents based on MOFs.

Adsorbent	Adsorption capacity of Pb^{2+} (mg/g)	Adsorption capacity of Cu^{2+} (mg/g)	Ref.
ZIF-67	1348.42	617.51	[23]
Cu(tpa)·GO	88	243	[18]
UiO-66-NH$_2$@CA	89	39	[25]
UiO-66@CA	81	31	[26]
Zn-MOFs/CNTs	1480	1620	This work

Reusability

Fig. 9. demonstrates that the Zn-MOFs/CNTs possess reversibility in the process of removing Pb^{2+} and Cu^{2+} ions. Typically, an adsorbent must possess stability and reusability to function effectively. Five rounds of adsorption/desorption were conducted to assess the reusability of the Zn-MOFs/CNTs, and the process was tracked using AAS. The sustained 98% removal efficiency over five cycles indicates that the Zn-MOFs/CNTs composite is potentially effective for industrial use.
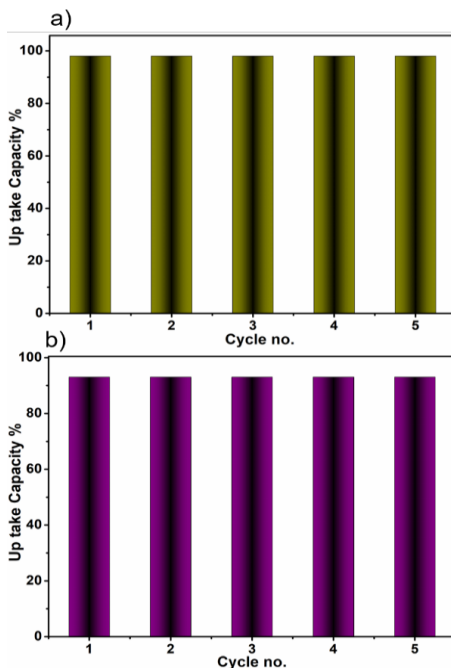

Fig. 9. Reusability experiments of Zn-MOFs/CNTs implemented with (a) Cu (II) ions, (b) Pb (II) ions.

Conclusions

In summary, composites used in MOFs exhibit significant potential for the efficient adsorption of heavy metal ions. This study introduces a novel Zn-MOFs/CNTs composite synthesized at room temperature. The Zn-MOFs/CNTs showed remarkable effectiveness in adsorbing Cu^{2+} and Pb^{2+} ions from water, achieving removal efficiencies of 98% and 93% within just 12 minutes. The maximum adsorption capacities for Cu^{2+} and Pb^{2+} ions were recorded at 1620 mg g^{-1} and 1480 mg g^{-1}, respectively. The Langmuir and pseudo-second-order rate models suggest that the Zn-MOFs/CNTs remove metal ions via a monolayer adsorption process, which is facilitated by the interaction between the active adsorption sites of the Zn-MOFs/CNTs and the Cu^{2+} and Pb^{2+} ions. This research demonstrates that MOFs combined with carbon nanotubes have exceptional adsorption capabilities for removing Cu^{2+} and Pb^{2+} ions from aqueous solutions.

Conflict of interests

⊠ The author(s) declare no competing interest.

_____

_____

References

[1]   L. Huang, M. He, B. Chen, B. Hu, Magnetic Zr-MOFs nanocomposites for rapid removal of heavy metal ions and dyes from water, Chemosphere. 199 (2018) 435–444. https://doi.org/10.1016/j.chemosphere.2018.02.019.

[2]   F. Zadehahmadi, N.T. Eden, H. Mahdavi, K. Konstas, J.I. Mardel, M. Shaibani, P.C. Banerjee, M.R. Hill, Removal of metals from water using MOF-based composite adsorbents, Environ. Sci. Water Res. Technol. 9 (2023) 1305–1330. https://doi.org/10.1039/d2ew00941b.

[3]   M.A. Hashim, S. Mukhopadhyay, J.N. Sahu, B. Sengupta, Remediation technologies for heavy metal contaminated groundwater, J. Environ. Manage. 92 (2011) 2355–2388.

[4]   V.K. Gupta, Application of low-cost adsorbents for dye removal–a review, J. Environ. Manage. 90 (2009) 2313–2342.

[5]   D. Mohan, K.P. Singh, V.K. Singh, Wastewater treatment using low cost activated carbons derived from agricultural byproducts—A case study, J. Hazard. Mater. 152 (2008) 1045–1053.

[6]   V. Meshko, L. Markovska, M. Mincheva, A.E. Rodrigues, Adsorption of basic dyes on granular activated carbon and natural zeolite, Water Res. 35 (2001) 3357–3366.

[7]   R. Zein, R. Suhaili, F. Earnestly, E. Munaf, Removal of Pb (II), Cd (II) and Co (II) from aqueous solution using Garcinia mangostana L. fruit shell, J. Hazard. Mater. 181 (2010) 52–56.

[8]   Y. Wang, Z. Gao, Y. Shang, Z. Qi, W. Zhao, Y. Peng, Proportional modulation of zinc-based MOF/carbon nanotube hybrids for simultaneous removal of phosphate and emerging organic contaminants with high efficiency, Chem. Eng. J. 417 (2021) 128063. https://doi.org/10.1016/j.cej.2020.128063.

[9]   Y.M. Moustafa, A.M. Al-Sabagh, S.A. Younis, M.M.H. Khalil, M.O. Abdel-Salam, Preparation of magnetic carbon nanotube nanocomposite for enhancing the separation of dissolved hydrocarbon from petroleum wastewater, J. Environ. Chem. Eng. 5 (2017). https://doi.org/10.1016/j.jece.2017.04.023.

[10]   S. Manikandan, N. Karmegam, R. Subbaiya, G. Karthiga Devi, R. Arulvel, B. Ravindran, M. Kumar Awasthi, Emerging nano-structured innovative materials as adsorbents in wastewater treatment, Bioresour. Technol. 320 (2021) 124394. https://doi.org/10.1016/j.biortech.2020.124394.

[11]   D.D. Chronopoulos, H. Saini, I. Tantis, R. Zbořil, K. Jayaramulu, M. Otyepka, Carbon Nanotube Based Metal-Organic Framework Hybrids From Fundamentals Toward Applications, Small. 18 (2022). https://doi.org/10.1002/smll.202104628.

[12]   M. Moharramnejad, A. Ehsani, R. Eshaghi, Zinc-based metal-organic frameworks : synthesis and recent progress in biomedical application, (2022) 3339–3354.

[13]   O.M. Rodriguez-Narvaez, J.M. Peralta-Hernandez, A. Goonetilleke, E.R. Bandala, Treatment technologies for emerging contaminants in water: A review, Chem. Eng. J. 323 (2017) 361–380. https://doi.org/10.1016/j.cej.2017.04.106.

[14]   <Recent developments on zincIJIII) metal-organic framework nanocarriers for physiological pH-responsive drug delivery Weicong, (n.d.).

[15]   Y. Wang, Z. Gao, Y. Shang, Z. Qi, W. Zhao, Y. Peng, Proportional modulation of zinc-based MOF/carbon nanotube hybrids for simultaneous removal of phosphate and emerging organic contaminants with high efficiency, Chem. Eng. J. 417 (2021) 128063. https://doi.org/10.1016/j.cej.2020.128063.

[16]   M. Li, Z. Zhang, Y. Yu, H. Yuan, A. Nezamzadeh-Ejhieh, J. Liu, Y. Pan, Q. Lan, Recent advances in Zn-MOFs and their derivatives for cancer therapeutic applications, Mater. Adv. 4 (2023) 5050–5093. https://doi.org/10.1039/d3ma00545c.

[17]   Y.M. Moustafa, A.M. Al-Sabagh, S.A. Younis, M.M.H. Khalil, M.O. Abdel-Salam, Preparation of magnetic carbon nanotube nanocomposite for enhancing the separation of dissolved hydrocarbon from petroleum wastewater, J. Environ. Chem. Eng. 5 (2017) 2240–2250. https://doi.org/10.1016/j.jece.2017.04.023.

[18]   S. Wang, B. Ye, C. An, J. Wang, Q. Li, H. Guo, J. Zhang, Exploring the Coordination Effect of GO@MOF-5 as Catalyst on Thermal Decomposition of Ammonium Perchlorate, Nanoscale Res. Lett. 14 (2019). https://doi.org/10.1186/s11671-019-3163-z.

[19]   Ata-ur-Rehman, S.A. Tirmizi, A. Badshah, H.M. Ammad, M. Jawad, S.M. Abbas, U.A. Rana, S.U.D. Khan, Synthesis of highly stable MOF-5@MWCNTs nanocomposite with improved hydrophobic properties, Arab. J. Chem. 11 (2018) 26–33. https://doi.org/10.1016/j.arabjc.2017.01.012.

[20]   Y. ping Wei, Y. wen Zhang, J.S. Chen, C. jie Mao, B.K. Jin, An electrochemiluminescence biosensor for p53 antibody based on Zn-MOF/GO nanocomposite and Ag+-DNA amplification, Microchim. Acta. 187 (2020) 1–9. https://doi.org/10.1007/s00604-020-04425-1.

[21]   F. Akbarzadeh, M. Motaghi, N.P.S. Chauhan, G. Sargazi, A novel synthesis of new antibacterial nanostructures based on Zn-MOF compound: design, characterization and a high performance application, Heliyon. 6 (2020) e03231. https://doi.org/10.1016/j.heliyon.2020.e03231.

[22]   M. del Rio, J.C. Grimalt Escarabajal, G. Turnes Palomino, C. Palomino Cabello, Zinc/Iron mixed-metal MOF-74 derived magnetic carbon nanorods for the enhanced removal of organic pollutants from water, Chem. Eng. J. 428 (2022) 131147. https://doi.org/10.1016/j.cej.2021.131147.

[23]   Z. Li, D. Pei, R. Tian, C. Lu, Screening the Specific Surface Area for Metal-Organic Frameworks by Cataluminescence, Chemosensors. 11 (2023). https://doi.org/10.3390/chemosensors11050292.

_____

_____

[24]   E. Rahimi, N. Mohaghegh, New hybrid nanocomposite of copper terephthalate MOF-graphene oxide: synthesis, characterization and application as adsorbents for toxic metal ion removal from Sungun acid mine drainage, Environ. Sci. Pollut. Res. 24 (2017) 22353–22360. https://doi.org/10.1007/s11356-017-9823-6.

[25]   Fabrication of metal-organic frameworks @ cellulose aerogels composite materials for removal of heavy metal ions in water, Carbohydrate Polymers, 205 (2019) 35–41, https://doi.org/10.1016/j.carbpol.2018.10.02.

_____